Proc. Natl. Acad. Sci. USA
Vol. 87, pp. 8257–8261, November 1990
Neurobiology

Effects of synapsin I and calcium/calmodulin-dependent protein kinase II on spontaneous neurotransmitter release in the squid giant synapse

(miniatures/facilitation/protein phosphorylation/phosphoproteins)

JEN-WEI. LIN*†, MUTSUYUKI SUGIMORI*†, RODOLFO R. LLINÁS*†‡, TERESA L. MCGUINNESS*§, AND PAUL GREENGARD*§

*Marine Biological Laboratory, Woods Hole, MA 02543; †Department of Physiology and Biophysics, New York University Medical Center, New York, NY 10016; and §Laboratory of Molecular and Cellular Neuroscience, The Rockefeller University, New York, NY 10021

Contributed by Paul Greengard, July 27, 1990

ABSTRACT **The molecular events that control synaptic vesicle availability in chemical synaptic junctions have not been fully clarified. Among the protein molecules specifically located in presynaptic terminals, synapsin I and calcium/calmodulin-dependent protein kinase II (CaM kinase II) have been shown to modulate evoked transmitter release in the squid giant synapse. In the present study, analysis of synaptic noise in this chemical junction was used to determine whether these proteins also play a role in the control of spontaneous and enhanced spontaneous transmitter release. Injections of dephosphorylated synapsin I into the presynaptic terminal reduced the rate of spontaneous and enhanced quantal release, whereas injection of phosphorylated synapsin I did not modify such release. By contrast CaM kinase II injection increased enhanced miniature release without affecting spontaneous miniature frequency. These results support the view that dephosphorylated synapsin I "cages" synaptic vesicles while CaM kinase II, by phosphorylating synapsin I, "decages" these organelles and increases their availability for release without affecting the release mechanism itself.**

Synapsin I, a neuron-specific protein present in nerve terminals (1), has recently been shown to be a powerful modulator of neurotransmitter release (2). This protein is known to adhere to synaptic vesicles and may cross-link them to the cytoskeleton at or near the active zone in presynaptic terminals (3). Synapsin I is a substrate for calcium/calmodulin-dependent protein kinase II (CaM kinase II) (4). The affinity of synapsin I for synaptic vesicles (5) and for actin (3) is reduced after phosphorylation by CaM kinase II. The physiological role of synapsin I and CaM kinase II has been studied in the squid giant synapse (2) and in the goldfish Mauthner cell (6). The results from these studies indicated that transmitter release is inhibited if dephosphorylated synapsin I is injected into the presynaptic terminal, but that it is not affected by injection of phosphorylated synapsin I (2, 6). Our results further indicated that CaM kinase II injections induced a significant increase of transmitter release (2).

Since voltage clamp studies showed that the amplitude of the presynaptic calcium current was not modified by the injection of any of these proteins (2), it was proposed that the phosphorylation of synapsin I by CaM kinase II allows the vesicles to be freed from a bound or "caged" state and to become available for release (2, 7–9). Consistent with this hypothesis, recent video microscopic observations indicate that organelle movements in the squid axoplasm are markedly reduced after the addition of dephosphorylated synapsin I, but not after administration of phosphorylated synapsin I (10).

A corollary of this hypothesis is that spontaneous and enhanced quantal transmitter release may be subjected to the same type of regulation by synapsin I and CaM kinase II. In this report, noise analysis was used to demonstrate that, depending on its state of phosphorylation, synapsin I can regulate the availability of synaptic vesicles for release. CaM kinase II, while increasing evoked miniature release, did not affect spontaneous release, indicating that, as concluded in our previous study, this enzyme does not regulate the release mechanism itself (2). A short report has been published relating to the present findings (11).

MATERIALS AND METHODS

Electrophysiology. Squid (*Loligo pealii*) ≈4 inches long and obtained from the Marine Biological Laboratory (Woods Hole, MA) were used in these experiments. The isolation of the stellate ganglion and electrophysiological recording techniques have been described (12). The ganglion was perfused with artificial seawater buffered by Tris (423 mM NaCl/8.3 mM KCl/10 mM $CaCl_2$/50 mM $MgCl_2$/2 mM Tris, pH 7.2/0.001% H_2O_2) and maintained at room temperature (20°C). The presynaptic terminal was penetrated with two electrodes, one for pressure injection of proteins and one for monitoring membrane potential. The pressure injection electrode was also used to inject current in voltage clamp experiments (12). The postsynaptic electrodes were beveled to reduce their resistance (<1 MΩ) and thus optimize the signal/noise ratio. For voltage clamp experiments, sodium and potassium currents were blocked by bath application of 1 μM tetrodotoxin and 5 mM 3- or 4-aminopyridine, respectively.

Protein Preparation and Pressure Injection. The methodology used in the preparation and injection of synapsin I and CaM kinase II was the same as those reported in previous publications (2–4).

Noise Analysis. Noise analysis (13) was based on the assumption that the waveform of unitary synaptic potentials produced by the squid giant synapse may be approximated by the difference between two exponential functions (14):

$$F(t) = a[e^{-t/t_d} - e^{-t/t_r}], \quad [1]$$

where a is a scaling factor for the amplitude of unitary potential, t_d is the decay time constant, and t_r is the rise time constant. (Note that the waveform described by this equation

The publication costs of this article were defrayed in part by page charge payment. This article must therefore be hereby marked "*advertisement*" in accordance with 18 U.S.C. §1734 solely to indicate this fact.

Abbreviation: CaM kinase II, calcium/calmodulin-dependent protein kinase II.

‡To whom reprint requests should be addressed at: Department of Physiology and Biophysics, New York University Medical Center, 550 First Avenue, New York, NY 10016.

does not rise exponentially and its decay can be approximated by a single exponential time constant only when t is large.) This is a more realistic approximation than that used previously in this preparation (15), where a time course of instantaneous rise followed by a single exponential decay was used to approximate unitary potentials. In fact, under optimal recording conditions in small synapses where the input resistance of the postsynaptic axon was high, most of the unitary potentials had a close to symmetrical triangular waveform (11, 16, 17). We have successfully used this function to fit the waveform of averaged unitary synaptic potentials (13). The power spectrum derived from such a unitary potential time course is (14):

$$S(f) = 2na^2(t_d - t_r)^2/[(1 + 4\pi^2f^2t_d^2)(1 + 4\pi^2f^2t_r^2)], \quad [2]$$

where n is the rate of unitary release (events/sec); f is the frequency; and a, t_d, and t_r are the same as defined for Eq. 1. The variance produced by such unitary potentials is given by:

$$v = na^2(t_d - t_r)^2/2(t_d + t_r). \quad [3]$$

It is possible to substitute the variance (Eq. 3) into the power spectrum (Eq. 2) such that two unknown variables, n and a, can be eliminated.

$$S(f) = 4v(t_d + t_r)/[(1 + 4\pi^2f^2t_d^2)(1 + 4\pi^2f^2t_r^2)]. \quad [4]$$

This substitution simplifies the curve-fitting procedure for the power spectrum (see below).

Synaptic noise was recorded with a high-gain (×100), low-noise, ac-coupled amplifier filtered at 1.25 kHz (with a Butterworth filter) and was sampled at 2.5 kHz with a Nicolet digital oscilloscope. A typical episode contained 16,000 data points. The data were then transferred to a Macintosh II computer for noise analysis. Each episode was divided into segments of 1024 points and each segment was cosine tapered (18). To avoid loss of information due to the tapering, consecutive segments of data had a 50% overlap. Thus, a 16,000 data stretch resulted in 31 overlapping segments. Each segment was then fast Fourier transformed and the resultant power spectra were averaged. The effect of tapering on the magnitude of the power spectrum was corrected. The same procedure was applied to the background noise recorded after damaging the presynaptic terminal by overdriving the voltage clamp circuit, which resulted in a complete disappearance of synaptic transmission and a marked reduction of the synaptic noise recorded from the postsynaptic axon. After subtracting the power spectrum of the background noise from that of the synaptic noise, the characteristic frequency of the synaptic noise was obtained by using a curve-fitting program. The variance calculated from the data was first substituted into Eq. 4. The best fit was then obtained after searching systematically through a defined range of time constants, which produced realistic unitary potential waveforms. Any change in the power spectrum characteristic frequency was detected by comparing the values of the best-fit frequencies or comparing the time courses of the unitary potentials reconstructed from the characteristic frequencies. Since several possible combinations of time constants may produce similar unitary potential waveforms, both types of comparison were routinely used.

The noise analysis procedure was tested with simulated synaptic noise where the time course of the unitary current and the frequency of its occurrence were determined and its occurrence along the time axis was assigned randomly (13). In addition, various levels of background noise were added to the simulated data to determine the resolution of our procedure. The noise analysis procedure described above could reliably reconstruct the input parameters as long as the standard deviation of the background noise was less than twice that of the unitary potential amplitude. In practice, we rejected those experiments in which the background noise had a variance larger than 200 μV^2, assuming a unitary amplitude of 10 μV. When this procedure was applied to experimental data where different levels of transmitter release were evoked by presynaptic depolarizations, consistent frequency characteristics were obtained for each synapse. For example, rise time constants of 0.2–0.3 msec and decay time constants of 1.5–1.6 msec were consistently obtained from a synapse where the level of maximal transmitter release was >7 times larger than the minimal release level.

RESULTS

Effect of Dephosphorylated Synapsin I on Synaptic Noise. The voltage noise recorded in the postsynaptic axon at rest was similar to the spontaneous transmitter release initially described in the neuromuscular junction (19). In most trials, this synaptic noise was not stable but declined over time. An average decrease of 39% (n = 3) in the noise levels was seen 20 min after electrode penetration and injection of the vehicle solution (500 mM KCl/10 mM K_2HPO_4, pH 7.4). This decrease was presumably due to the initial injury caused by penetration of the presynaptic terminal by the electrode.

In contrast to the slow reduction of spontaneous synaptic noise noted above, the injection of dephosphorylated synapsin I produced a rapid and robust decline of this signal. The level of noise decrease is illustrated in the recordings shown in Fig. 1, where traces obtained at different times after the

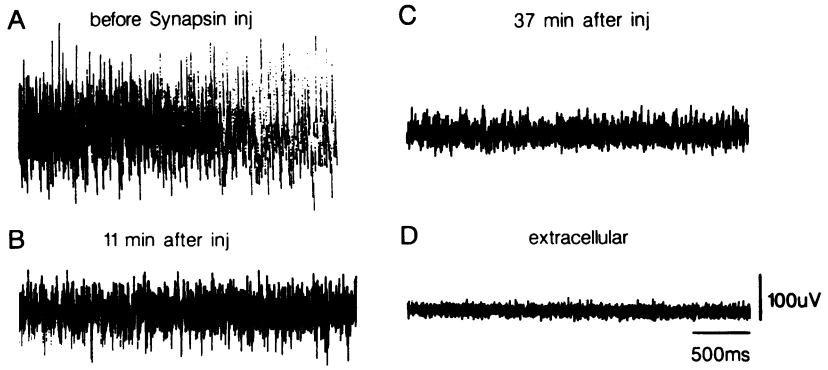

FIG. 1. Effect of injection of dephosphorylated synapsin I on spontaneous synaptic noise. (*A*) Control synaptic noise recorded 10 min after presynaptic penetration but immediately before injection. Synaptic noise recorded 11 min (*B*) and 37 min (*C*) after the injection. (*D*) Noise level recorded after the postsynaptic electrode was withdrawn from axon. All the traces were recorded under ac coupling and were low-pass filtered at 1.25 kHz.

protein injection are shown. The thickness of the traces reflects the level of spontaneous release (Fig. 1 *A–C*). The extracellular noise trace is shown in Fig. 1*D* to illustrate the resolution of the recording system.

Quantification of the level of synaptic noise was determined as the variance of the recorded traces. A plot of noise level over time is shown in Fig. 2*A*, where the noise level was normalized to the variance recorded before the injection. Because the rate of decline of the synaptic noise recorded after injection of phosphorylated synapsin I or the vehicle solution was the same as the preinjection levels, these rates served as controls for the effect of dephosphorylated synapsin I injection. After injection of dephosphorylated synapsin I the average noise level was reduced to 21% of the control after 20 min (Fig. 2*A*, open squares), whereas after injection of phosphorylated synapsin I or vehicle the noise level was 70–90% of the control value at that time (Fig. 2*A*, solid squares, open circles). That the reduction by dephosphorylated synapsin I was not due to damage of the presynaptic terminal was demonstrated by the fact that the noise recorded immediately after the injections (Fig. 2*A*, time 0) was identical to the preinjected level (Fig. 2*A*, −10 to 0 min). Normally, damage of a presynaptic terminal due to injection is associated with a marked increase in spontaneous noise. In five experiments in which spontaneous and evoked release were monitored simultaneously, the injection of dephosphorylated synapsin I was accompanied by a parallel reduction of both types of transmitter release. Since the spontaneous noise represented a significant fraction of the evoked noise (Fig. 2*B*), the true time course of the inhibition of evoked release was obtained by subtracting the spontaneous noise from the evoked noise. The corrected time course (Fig. 2*C*) has a slightly slower, but statistically insignificant, decline compared with that of the spontaneous noise (Fig. 2*B*). This curve is very similar to that measured from the amplitude of the postsynaptic potentials after injection of dephosphorylated synapsin I (2) and presumably reflects the time course of diffusion of dephosphorylated synapsin I into the terminal.

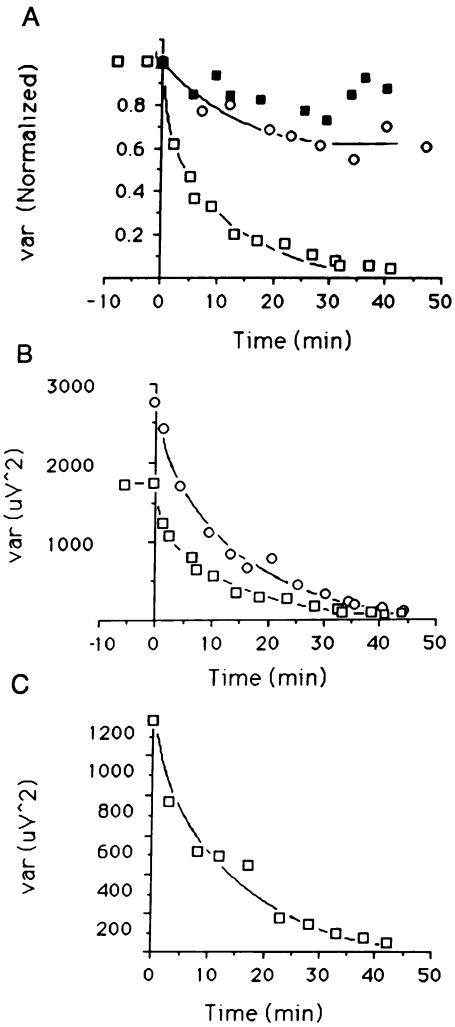

FIG. 2. Decline of synaptic noise produced by injection of dephosphorylated synapsin I. (*A*) The reduction of synaptic noise after injection of dephosphorylated synapsin I (□) was much more rapid than that produced by injection of the vehicle alone (○) or of phosphorylated synapsin I (■). The vehicle solution consisted of 500 mM KCl/10 mM K_2HPO_4, pH 7.4. The level of synaptic noise after presynaptic penetration was monitored for ≈10 min before the protein was pressure injected. Two data points representing 8 and 3 min before the injection are shown in the negative time scale. The noise for each experiment was normalized to the variance recorded at time 0 after background noise subtraction. (*B*) Comparison of noise decline recorded from evoked (○) and spontaneous (□) noise. The evoked noise was activated by a depolarization of 15 mV, with a duration of 2 sec, from a holding potential of −70 mV. (*C*) The time course of inhibition of evoked transmitter release produced after the injection. The data points were obtained by subtracting the variance of spontaneous noise from that of evoked noise.

Since the frequency of unitary events is linearly related to the variance, and the amplitude of the unitary events is unlikely to be changed by injection of dephosphorylated synapsin I (6), the accelerated decline of synaptic noise after the injection is most likely due to a reduction in the rate of spontaneous release. With the assumption of a unitary amplitude of 10 μV, the spontaneous release in the synapse illustrated in Figs. 2 and 3 declined from 36,000 quanta/sec before the injection to 1770 quanta/sec 22 min after the injection. (The calculations were based on Eq. 3, where the time constants were derived from noise spectrum fitting and the variance was obtained from the data.) The validity of the assumption that the shape and amplitude of the unitary events do not change is supported by the observation that power spectra before and after injection of dephosphorylated synapsin I exhibited identical characteristics. This is shown in Fig. 3 *A–C*, where power spectra obtained before and after injection of dephosphorylated synapsin I are plotted for comparison. The data in Fig. 3*A* are unprocessed power spectra—i.e., the background noise had not been subtracted. The spectra after the correction and their best fits are shown in Fig. 3*C*. In this case, both control and experimental spectra exhibit similar frequency characteristics. To illustrate the stability of the frequency characteristics better, the best-fit spectra at various times after injection of dephosphorylated synapsin I are plotted together in Fig. 3*B*. For example, the rise time constant was 0.66 msec before the protein injection and 0.74 msec 11 min after the injection. The decay time constant also remained stable at 0.75 msec and 0.82 msec before and after injection, respectively. Their similarity was demonstrated by superimposing the unitary events reconstructed from the time constants (Fig. 3*D*).

Effect of CaM Kinase II on Synaptic Noise. The decline of spontaneous synaptic noise after CaM kinase II injection was similar to that produced by vehicle injection (Fig. 4*A*) and by injection of phosphorylated synapsin I (data not shown). On the average, the spontaneous noise declined by 42% ($n = 4$) 20 min after the injection, a value similar to that obtained from vehicle and phosphorylated synapsin I experiments (39%). In contrast, evoked release increased gradually after CaM kinase II injection (Figs. 4*B* and 5). The increase in evoked release was indicated by an elevation of noise that occurred during the presynaptic depolarizing clamp pulse. This is illustrated in Fig. 5 *A* and *B*, where the same presynaptic depolarization produced a larger noise after CaM kinase II injection. Traces in Fig. 5 *C* and *D* show the same

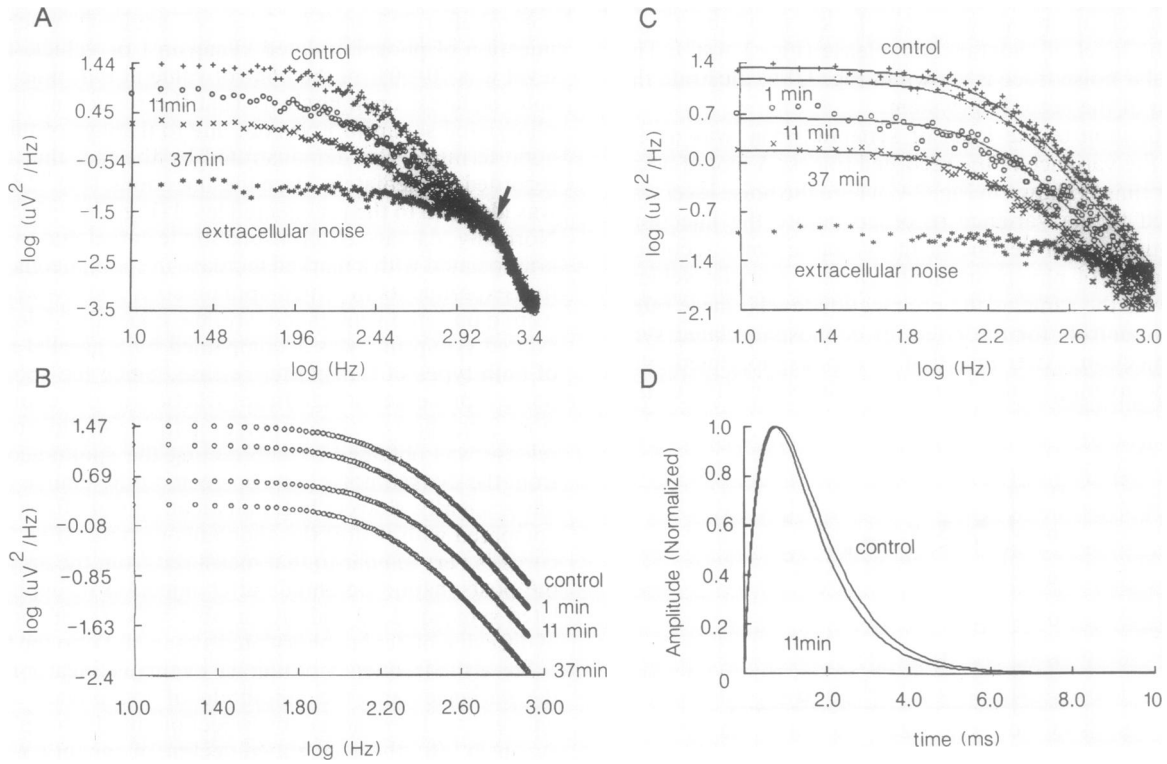

FIG. 3. Effect of injection of dephosphorylated synapsin I on the frequency characteristics of spontaneous noise. (*A*) Power spectra before background noise was subtracted. A sharp bend at ≈1.25 kHz (arrow) indicates the corner frequency of the low-pass filter. The power spectra obtained before (+), 11 min (○), and 37 min (×) after injection are plotted together with the spectrum of extracellular noise (*). The spectrum obtained 1 min after injection was not included in *A* because it was too close to the control spectrum; however, it was included in *B*. The extracellular spectrum indicates that the noise of the recording system had a constant power up to 1 kHz. (*B*) The noise spectra reconstructed from the best fits of corrected power spectra at the indicated times. (*C*) Example of the power spectrum fitting. The data shown in *A* were first corrected by subtracting the spectral density of the background noise and then plotted up to 1 kHz. The best fits of these spectra are shown as solid lines. (*D*) Comparison of the reconstructed miniature potential waveform obtained before and after injection of dephosphorylated synapsin I. The characteristic frequencies of the best fit were first converted to corresponding time constants. Eq. 1 was then used to create the miniature potential time course and the amplitudes of the miniature potentials were then scaled to the same height for ease of comparison.

data at a higher time resolution. Furthermore, injection of CaM kinase II produced a parallel shift in the power spectrum due to an increased release rate, without changing the frequency characteristics (Fig. 5 *E* and *F*). The insensitivity of spontaneous release to CaM kinase II injection suggests that the resting level of intracellular calcium was not high enough to substantially activate this enzyme.

DISCUSSION

The results presented in this report are in agreement with our preliminary findings (11) and with data recently published on Mauthner cell junctions (6). The present results demonstrate that the injection of dephosphorylated synapsin I inhibits spontaneous transmitter release in a manner similar to the decrease in the evoked release. Furthermore, CaM kinase II

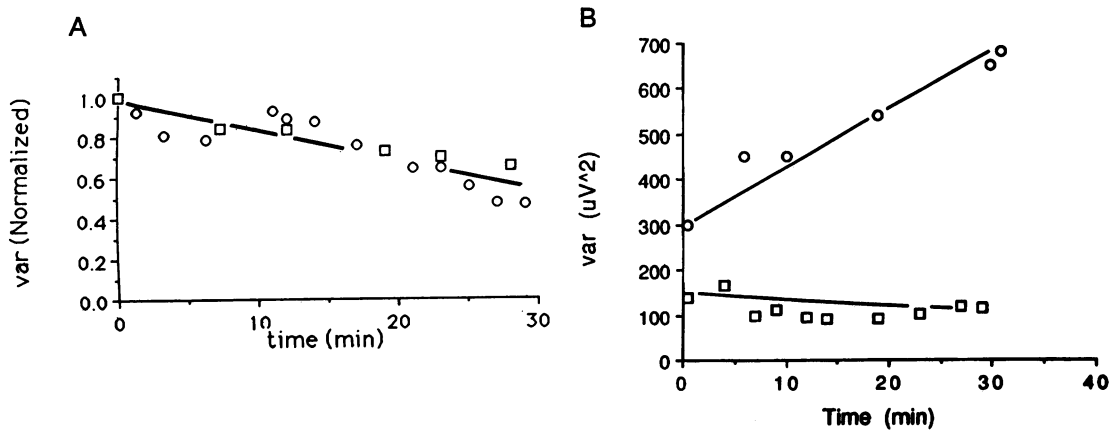

FIG. 4. Effect of CaM kinase II injection on evoked and spontaneous noise. (*A*) The decline of spontaneous noise after CaM kinase II injection (○) was not significantly different from that after vehicle injection (□). The method of variance normalization was identical to that used in Fig. 2. The control synaptic noise level, at time 0, was 1000 mV^2 for blank injection and 700 mV^2 for CaM kinase II injection. (*B*) Evoked noise (○) increased continuously after the injection, while spontaneous noise (□) remained stationary. The evoked noise was activated by a 15-mV pulse, with a duration of 2 sec, depolarized from a holding potential of −70 mV after background noise subtraction (*A* and *B* were obtained from different synapses).

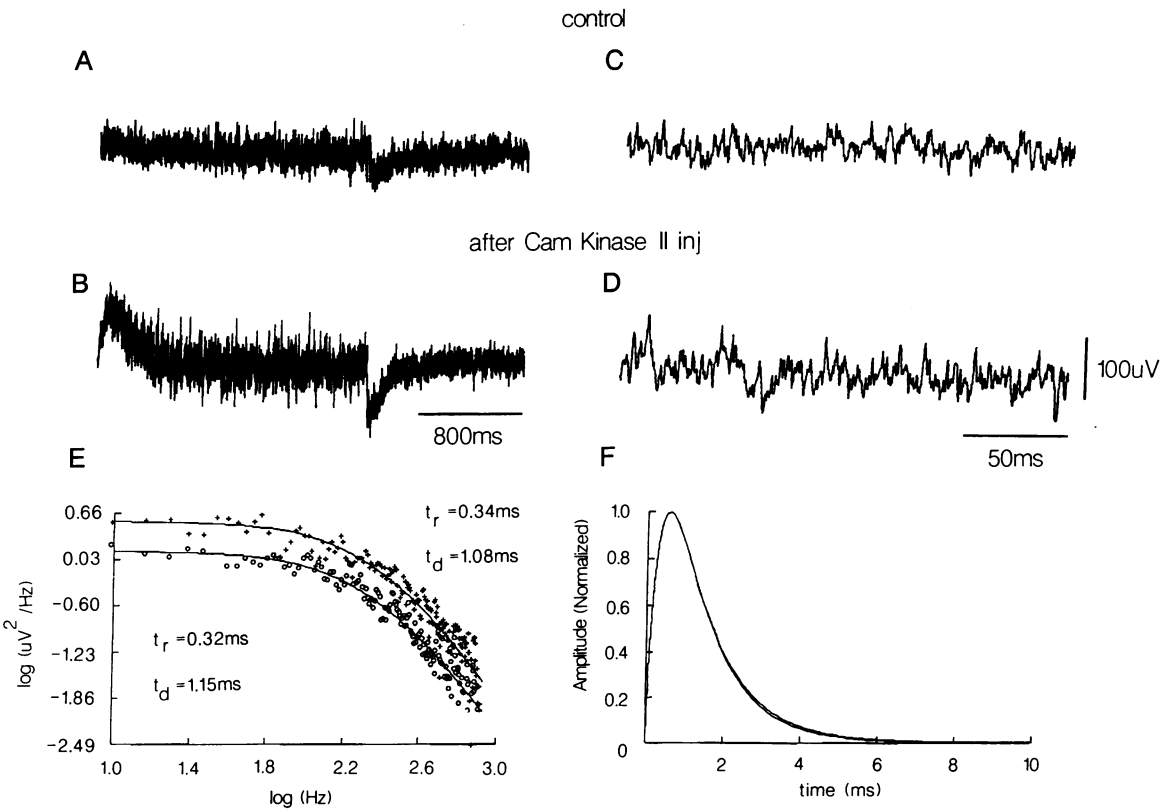

FIG. 5. CaM kinase II injection did not change the characteristic frequencies of the evoked release. Traces of evoked synaptic noise recorded before (*A* and *C*) and after (*B* and *D*) CaM kinase II injection are illustrated at slow (*A* and *B*) and fast (*C* and *D*) time scales. The presynaptic voltage clamp pulse had a duration of 2 sec. Its make and break times are identified by the fast transient due to the ac-coupled recording (*B*). (*E*) Power spectra and their best fits obtained from the examples shown in *A* (○) and *B* (+). The time constants derived from their characteristic frequencies were t_r = 0.32 msec and t_d = 1.15 msec before injection and t_r = 0.34 msec and t_d = 1.08 msec after CaM kinase II injection. These time constants were used to reconstruct the miniature potential waveforms shown in *F*. Note that these two waveforms were similar. The procedure for creating these waveforms is outlined in the legend to Fig. 3.

injection increased enhanced miniature release without affecting spontaneous release. The present findings lend additional support to the proposed role of the CaM kinase II/synapsin I pathway—namely, that synapsin I molecules limit the availability of synaptic vesicles while CaM kinase II can increase the availability of these vesicles for release (2). In support of this hypothesis, presynaptic terminal voltage clamp experiments showed that injection of synapsin I or CaM kinase II did not change presynaptic I_{Ca} (2). The changes of excitatory postsynaptic potential amplitudes seen after these injections, therefore, are most likely due to a change in the availability of synaptic vesicles (2). This interpretation is consistent with the hypothesis that dephosphorylated synapsin I cross-links synaptic vesicles to cytoskeleton components such as actin (3). These latter experiments define a physical counterpart for vesicle availability. Specifically, synaptic vesicles need to be dissociated from a lattice made of synapsin I, synaptic vesicles, and actin before they can move to the release sites where vesicular fusion and transmitter release occur. Noise analysis performed in the present study indicates that regulation of the availability of synaptic vesicles by synapsin I applies to both spontaneous and evoked release. The more prominent role of CaM kinase II in evoked than in spontaneous release is probably due to the resting free calcium concentration being too low to cause a marked activation of the injected CaM kinase II. However, it is conceivable that the resting free calcium may activate enough CaM kinase II to free vesicles from their caged state, but these freed vesicles may not take part in spontaneous release.

This research was supported by a Medical Scientist Training Fellowship GM-07205 (T.L.M.); U.S. Public Health Service Grants NS-14014 (R.R.L.), MH-06944 (P.G.), and NS-21550 (P.G.); and U.S. Air Force Office of Scientific Research Grant 85-0368 (R.R.L.)

1. DeCamilli, P., Cameron, R. & Greengard, P. (1983) *J. Cell Biol.* **96**, 1337–1354.
2. Llinás, R., McGuinness, T., Leonard, C. S., Sugimori, M. & Greengard, P. (1985) *Proc. Natl. Acad. Sci. USA* **82**, 3035–3039.
3. Bahler, M. & Greengard, P. (1987) *Nature (London)* **326**, 704–707.
4. McGuinness, T., Lai, Y. & Greengard, P. (1985) *J. Biol. Chem.* **260**, 1696–1704.
5. Huttner, W. B., Schiebler, W., Greengard, P. & DeCamilli, P. (1983) *J. Cell Biol.* **96**, 1374–1388.
6. Hackett, J. T., Cochran, S. L., Greenfield, L. J., Brosius, D. C. & Ueda, T. (1990) *J. Neurophysiol.* **63**, 701–706.
7. Greengard, P., Browning, M. D., McGuinness, T. L. & Llinás, R. (1987) *Adv. Exp. Med. Biol.* **221**, 135–153.
8. DeCamilli, P. & Greengard, P. (1986) *Biochem. Pharmacol.* **35**, 4349–4357.
9. DeCamilli, P., Benfenati, F., Valtorta, F. & Greengard, P. (1990) *Annu. Rev. Cell Biol.*, in press.
10. McGuinness, T., Brady, S., Gruner, J., Sugimori, M., Llinás, R. & Greengard, P. (1989) *J. Neurosci.* **9**, 4138–4149.
11. Llinás, R., Sugimori, M., Lin, J. W., McGuinness, T. & Greengard, P. (1988) *Biol. Bull.* **175**, 307.
12. Llinás, R., Steinberg, I. Z. & Walton, K. (1981) *Biophys. J.* **33**, 289–321.
13. Lin, J. W., Sugimori, M. & Llinás, R. (1988) *Biol. Bull.* **175**, 30.
14. Verveen, A. A. & DeFelice, L. J. (1974) *Prog. Biophys. Mol. Biol.* **28**, 189–265.
15. Augustine, G. J. & Eckert, R. (1984) *J. Physiol. (London)* **346**, 257–271.
16. Miledi, R. (1967) *J. Physiol. (London)* **192**, 379–406.
17. Mann, D. W. & Joyner, R. W. (1978) *J. Neurobiol.* **9**, 329–335.
18. Bendat, J. S. & Piersol, A. G. (1986) *Random Data: Analysis and Procedure* (Wiley-Interscience, New York).
19. Fatt, P. J. & Katz, B. (1952) *J. Physiol. (London)* **117**, 108–128.